

# A New Stealthy Target Detection based on Stratospheric Balloon-borne Radar System

M. Barbary, F.F. Yang

Col. of Electronic and Information Engineering  
Nanjing Uni. of Aeronautics & Astronautics  
Nanjing 210016, China

P. Zong

Col. of Astronautics  
Nanjing Uni. of Aeronautics & Astronautics  
Nanjing 210016, China

**Abstract**—A novel detection for stealthy target model F-117A with a higher aspect vision is introduced by using Stratospheric Balloon - borne Bistatic radar system. The potential problem of proposed scheme is platform instability impacted on the balloon by external wind force. The flight control system is studied in detail under typical random process, which is defined by Dryden turbulence Spectrum. To accurately detect the stealthy target model, a real Radar Cross Section (RCS) based on physical optics (PO) formulation is applied. The detection of proposed scheme has been improved due to increasing PO – scattering field of stealthy model with higher aspect angle comparing to the conventional Ground -based system. Simulations demonstrate that proposed scheme gives much higher location accuracy and reduces location errors.

**Keywords**—stealthy RCS; bistatic balloon-borne radar; PO method

## I. INTRODUCTION

The complexity of stealth target detection is not only related to the target itself, but also influenced by the electromagnetic environment [1]. The countering-stealth technologies are increasingly relevant, and research in this field is ongoing around the world. Stealth technology mostly focuses on defeating conventional ground-based detection radar. Thus, the success of counter stealth endeavors is focused mostly on novel and unique air defense infrastructure configurations. The Radar Cross Section (RCS) is an important evaluation criterion of aircraft's stealthy performance, the envelope of the backscatter from stealthy target varies rapidly with aspect angle. The shaping of stealthy objects to reduce the backscattered energy towards the radar is believed to be less effective when bistatic radar is used [2].

Several researches deal with improving stealthy target detection and tracking based on Ground-based bistatic radar system [2-4]. These researches didn't evaluate Bistatic radar sensitivity and performance of stealthy target with a higher aspect vision. Since the Bistatic radar system might be mounted on higher altitude platforms to achieve a larger probability of detecting stealthy target, the Bistatic radar sensitivity will be improved due to increasing the scattered field of stealthy target with higher altitude. In this paper, we investigate a novel technique for stealthy target detection based on Balloon-borne bistatic radar system. The stations are positioned in the stratosphere about 21 km above the Earth and kept stable in a sphere of radius of 0.5 km [5]. To achieve high location accuracy for stealthy target, the proposed scheme uses

a physical optics method (PO) to predict the real RCS of stealthy target. This will better represent the actual situation of the stealthy target detection. One of the open research issues is whether the platforms positional instability due to sudden gusts of stratospheric winds. In the aerospace field, the study of turbulence effects is of fundamental importance in a lot of different aspects [6]: such as improvements of the aerodynamic and structural analysis, prediction of expected behavior of a balloon-borne platform under various levels of turbulence, evaluation of the stability of onboard sensing equipment, and so on. Numerous turbulence models are enumerated and described. The most commonly adopted model to study the impact of the turbulent wind gust on the balloon-borne is the Dryden model. According to this model, the atmospheric turbulence is modeled as a random velocity process added by balloon-borne velocity vector described in a body-fixed Cartesian coordinate system.

The rest of this paper is organized as follows. In Section 2, we present balloon positional instability analysis and random wind mathematical model. Performance of the proposed scheme is evaluated via computer simulation in Section 3, followed by the conclusion in Section 4.

## II. BALLOON POSITIONAL INSTABILITY ANALYSIS

The general dynamic equations of a stratospheric balloon platform are derived for flight over flat and non-rotating Earth, considering buoyancy, added mass and relevant conceptual design data of the stratospheric platform. To include the effect of jet stream as a moving wind field, the dynamic equations of motion can be derived in the relative wind-axes, inertial wind-axes, or body-axes coordinate systems [7]. The relative wind-axes system is more convenient than other coordinate systems because it expresses the wind-effect terms explicitly, bringing easier understanding. Fig. 1 illustrates the relationship between horizontal wind vector, airspeed velocity vector, and local (Earth-fixed) velocity of the platform. The wind-relative velocity vector is defined by airspeed  $V$ , flight path angle  $\gamma$ , and heading  $\psi$ . From Fig. 1, the inertial flight velocity with respect to the local ENU frame is determined as:

$$\begin{aligned} V_I &= V + W = \dot{x}_i u + \dot{y}_i e + \dot{z}_i n \\ &= V \sin \gamma u + (V \cos \gamma \sin \psi + W_E) e + (V \cos \gamma \cos \psi + W_N) n \\ &= V_I \sin \gamma_I u + V_I \cos \gamma_I \sin \psi_I e + V_I \cos \gamma_I \cos \psi_I n \end{aligned} \quad (1)$$

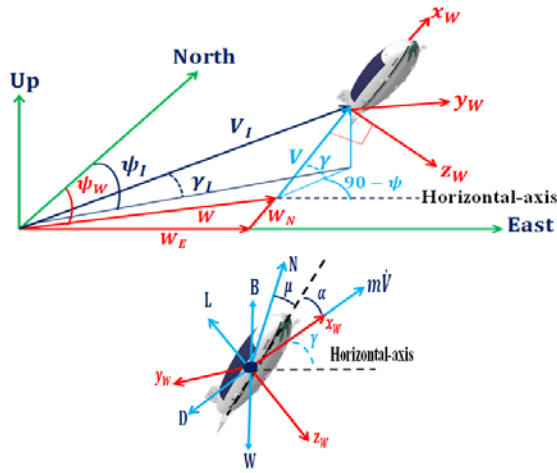


FIGURE I. BALLOON VELOCITY IN WIND FRAMES UNDER EXTERNAL FORCES ACTING.

The Dryden model is one of the most useful and tractable models for atmospheric turbulence [7]. To define it we need a body-fixed reference frame attached to the gravity centre of balloon-borne which moves with the target. The x-axis is on the position of motion direction, y-axis is on position along the wings, and z-axis is perpendicular to the balloon-borne plane. Then, the turbulence is modeled by adding some random components to balloon-borne velocity defined in the body-fixed coordinate system. An important consideration in this paper is the effect of steady-state horizontal winds. The horizontal wind velocity vector is defined as:

$$W_H = W \sin \psi_w e + W \cos \psi_w n = W_E e + W_N n \quad (2)$$

In Dryden model that continuous-time random processes are modeled as zero-mean, Gaussian-distributed processes whose PSD have analytic form given by [7]:

$$S_e(\omega) = \sigma_e^2 \frac{L_e}{\pi V_0} \frac{1}{1 + \left(\frac{L_e}{V_0} \omega\right)^2};$$

$$S_n(\omega) = \sigma_n^2 \frac{L_n}{2\pi V_0} \frac{1 + 3\left(\frac{L_n}{V_0} \omega\right)^2}{\left[1 + \left(\frac{L_n}{V_0} \omega\right)^2\right]^2} \quad (3)$$

where  $V_0$  is the gust wind speed in the balloon-borne system. The parameters  $\sigma_e^2$  and  $\sigma_n^2$  depend on the level of turbulence to be simulated and are selected accordingly. Parameters  $L_e$  and  $L_n$  are the scale lengths for the PSDs and depend on the flight altitude. The mean wind velocity at the altitude of 21km varies between -15 to +15 m/s. Fig. 2 shows the PSDs of (4) and (5) for  $\sigma_e = \sigma_n = \sigma_w = 15$  m/s,  $L_e = L_n = 533.54$  m, and  $V_0 = 15$  m/s. To reflect higher level of turbulence, the curves would be multiplied by the desired values of  $\sigma_e^2$  and  $\sigma_n^2$ .

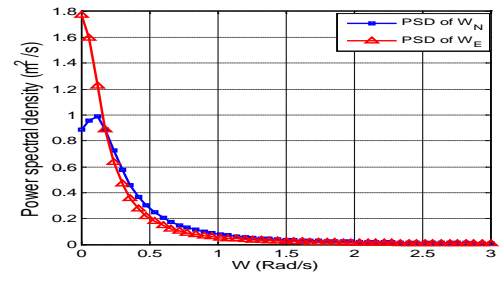


FIGURE II. PSD OF DRYDEN VELOCITY PROCESSES.

From (2) and (3), simulation model of wind can be written as:

$$\dot{W}_E + \frac{V_0}{L_e} W_E = \sqrt{\frac{2V_0}{L_e}} \xi_e, \quad \dot{W}_1 + \frac{V_0}{L_n} W_1 = (\sqrt{3} - 1) \sqrt{\frac{V_0}{L_n}} \xi_n,$$

$$\dot{W}_N + \frac{V_0}{L_n} W_1 + \frac{V_0}{L_n} W_N = \sqrt{\frac{3V_0}{L_n}} \xi_n \quad (4)$$

where  $W_1$  is the transition variable for calculating the wind field model,  $\xi_e$  and  $\xi_n$  are the random variables subject to normal distribution  $N(0, \sigma_w^2)$ . The external forces acting on Balloon-borne platform include aerodynamic lift (L) and drag (D), thrust (T), weight (W) and buoyancy (B). We also consider a generic lateral force (N), which may be generated by any means, such as rolling the lift vector through a small angle,  $\phi$ , or applying lateral thrust. A free-body diagram of the forces in x-z plane is shown in Fig. 1. The equations of motion are described by equating the time derivative of the momentum vector with the sum of external forces.

$$\sum F = \frac{d}{dt} (M V_i)$$

$$= [(B - W) \sin \gamma + T \cos(\alpha + \mu) - D] \hat{x} + N \hat{y} + [(W - B) \cos \gamma - L - T \sin(\alpha + \mu)] \hat{z} \quad (5)$$

Finally, solving the simultaneous algebraic equations for the derivatives  $\dot{V}$ ,  $\dot{\gamma}$ , and  $\dot{\psi}$ , the force equilibrium equations can be represented as

$$\dot{V} = \frac{(T \cos \alpha - D) - (mg - B) \sin \gamma}{m_T} - \dot{w}_{wx} \quad (6a)$$

$$\dot{\gamma} = \frac{(T \sin \alpha + L) \cos \phi - (mg - B) \cos \gamma}{m_T V} + \frac{\dot{w}_{wz} \cos \phi + \dot{w}_{wy} \sin \phi}{V} \quad (6b)$$

$$\dot{\psi} = \frac{(T \sin \alpha + L) \sin \phi}{m_T V \cos \gamma} + \frac{\dot{w}_{wz} \sin \phi - \dot{w}_{wy} \cos \phi}{V \cos \gamma} \quad (6c)$$

where

$$\dot{w}_{wx} = \dot{w}_N \cos \gamma \cos \psi + \dot{w}_E \cos \gamma \sin \psi \quad (7a)$$

$$\dot{w}_{wy} = \dot{w}_N (\sin \phi \sin \gamma \cos \psi - \cos \phi \sin \psi) + \dot{w}_E (\sin \phi \sin \gamma \sin \psi + \cos \phi \cos \psi) \quad (7b)$$

$$\dot{w}_{wz} = \dot{w}_N (\cos \phi \sin \gamma \cos \psi + \sin \phi \sin \psi) + \dot{w}_E (\cos \phi \sin \gamma \sin \psi - \sin \phi \sin \psi) \quad (7c)$$

### III. SIMULATION RESULTS

#### A. Instability of Balloon- Borne Receiver According to Wind Speed Results

For all problems considered, the ideal balloon position is fixed at  $(X = 150 \text{ Km}, Y = 100 \text{ Km}, Z = 21 \text{ Km})$  from the ground-based transmitter. The balloon is initialized by flying at 1m/s airspeed. With solving the optimal control problems, we neglect the contribution from centripetal acceleration, assuming acceleration is constant in the ENU farm, with a magnitude of  $0.029 \text{ m/s}^2$ . The simulation displays the positional instability of the balloon- borne receiver according to the horizontal wind speed, taking 250 seconds of random wind as an example,  $\sigma_w$  is of 15 m/s shown in Fig. 3(a). It is clear that the mean wind velocity at altitude of 21 Km varies randomly between  $-15$  to  $+15 \text{ m/s}$ . Fig.3 (b) shows the comparison between the ideal position and unstable balloon position in X-direction and Y-direction. It is clear that the balloon suspends in the stratosphere about 21 km above the Earth and extends in a sphere of 0.5 km radius.

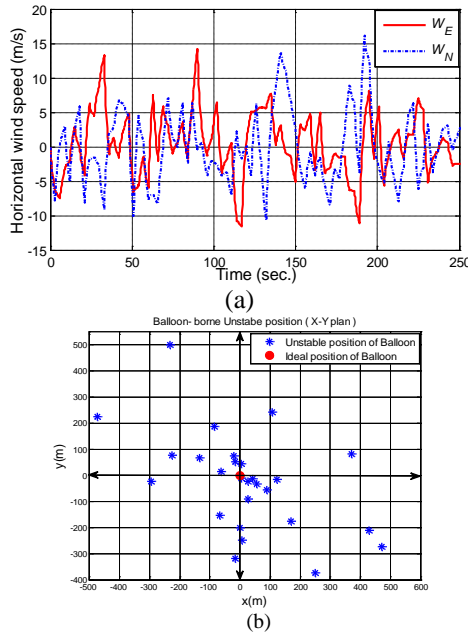


FIGURE III. SIMULATION OF RANDOM HORIZONTAL WIND SPEED AND THE COMPARISON BETWEEN THE IDEAL POSITION AND UNSTABLE BALLOON POSITION.

#### B. Establishing the Stealthy Target Model and Detection Results

A stealth target model implemented by PO approximation is used to detect the RCS[8]. The scientific computational features of MATLAB and GUI functions provide an efficient

calculation of stealthy RCS. Fig. 4(a) shows the geometry model and scatters of stealth target F-117A in the range of  $(0 \leq \theta \leq 360)$  and  $(0 \leq \phi \leq 360)$ . Fig. 4(b) shows 3-D RCS of the stealth target in bistatic system. A comparison of 2-D bistatic RCS with different aspect angle  $(\theta)$  according to the altitude of bistatic receiver is demonstrated in Fig. 5 (a). We further assume that the incident wave is  $(\theta$ -polarized), frequency is 3GHz and elevation angle takes two values  $(\theta = 80$  and  $120$  degree) while azimuth angle  $(\phi)$  between the horizon and observation direction varies from  $(0$  to  $360$  degrees). It is clear that the RCS with a higher aspect angle in Balloon-borne radar is better than with lower aspect angles in ground-based bistatic system. Fig. 5(b) shows the (RMSE) in range of stealthy target detection. It shows that RMSE of proposed scheme under instable position has been improved comparing to the conventional Ground-based radar by increasing scatterer RCS of stealth model with higher aspect angle. Fig. 6(a) presents the contour plots of GDOP values for real stealth RCS in different radar geometrical structures. The GDOP of Balloon-borne radar has been improved on conventional ground-based radar by higher aspect vision. Fig. 6(b) show a comparison between tracking of stealth target using proposed scheme and the conventional ground system.

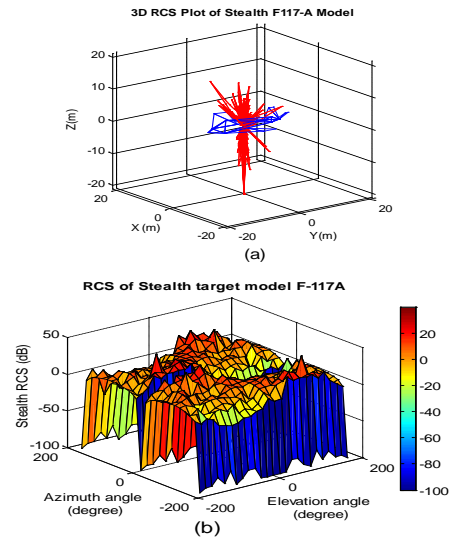


FIGURE IV. BISTATIC RCS OF THE STEALTHY TARGET BASED ON F-117A IN 3-D.

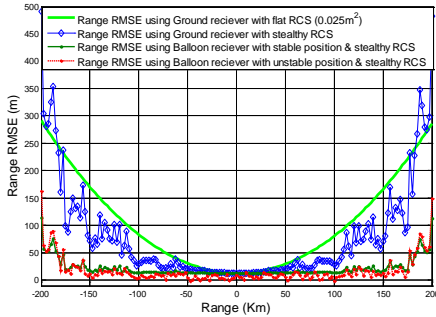
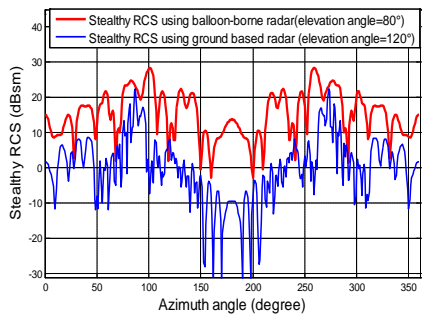


FIGURE V. A COMPARISON BETWEEN THE (RMSE) OF STEALTHY TARGET DETECTION WITH PROPOSED SCHEME AND CONVENTIONAL SYSTEM.

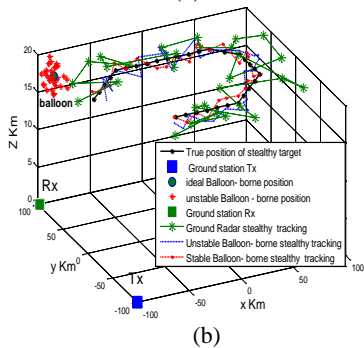
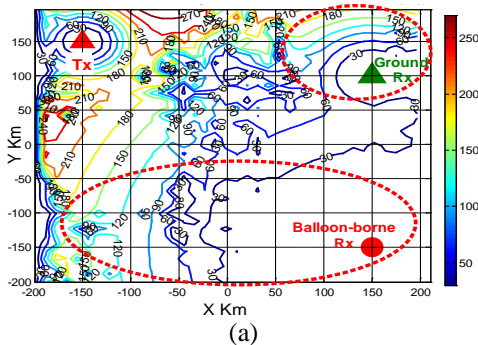


FIGURE VI. (A) THE GDOP (M) COMPARISON OF BALLOON-BORNE AND CONVENTIONAL GROUND-BASED BISTATIC SYSTEM. (B) THE COMPARISON BETWEEN THE TRACKING .

#### IV. CONCLUSION

An improvement of stealth RCS detection with a higher aspect vision is presented. The stratospheric Balloon positional instability due to random wind is considered. The results revealed that proposed scheme demonstrates higher location

accuracy than conventional Ground-based system. It is clear that Bistatic radar sensitivity of proposed scheme has been improved due to increasing scatterer RCS of stealth model with a higher aspect angle which predicted by PO method. The comparison between tracking of stealth target using proposed scheme and conventional system is introduced. The GDOP of proposed scheme has been improved due to decreasing the RMSE of balloon radar system comparing to the conventional system. Finally the proposed system has better performance at almost all time intervals.

#### ACKNOWLEDGMENTS

This work is supported by China National Found of “863 Project”, Ref. 2013AA7010051.

#### REFERENCES

- [1] X. CHEN, J. GUAN, N. LIU, Y. HE, Maneuvering Target Detection via Radon-Fractional Fourier Transform-Based Long Time Coherent Integration, *IEEE Trans. Signal Process.*, 2014, vol. 62, no. 4, p. 939–953.
- [2] H. KUSCHEL, J. HECKENBACH, ST. MULIER, R. APPEL, Countering Stealth with Passive, Multi-static, Low Frequency Radars, *IEEE Aerospace and Electronic Systems Magazine*, 2010, vol.25, no.9, p. 11 - 17.
- [3] D. HOWE, Introduction to the basic technology of stealthy aircraft: Part 2- Illumination by the enemy (active considerations), *Journal of Engineering for Gas Turbines and Power*, 1991, vol.113, no. 1, p. 80-86.
- [4] H. EL - KAMCHOUCY, K. SAADA, A. HAFEZ, Optimum Stealthy Aircraft Detection Using a Multistatic Radar, *ICACT Transactions on Advanced Communications Technology (ICACT-TACT)*, 2013, vol. 6, no. 2, p. 337-342.
- [5] D.I. AXIOTIS, M.E. THEOLOGOU, E.D. SYKAS, The Effect of Platform Instability on the System Level Performance of HAPS UMTS, *IEEE Communications Letters*, 2004, vol. 8, no.2, p. 111-113.
- [6] S. FORTUNATI, A. FARINA, F. GINI, A. GRAZIANO, M.S. GRECO, S. GIOMPAPA, Impact of Flight Disturbances on Airborne Radar Tracking, *IEEE Transactions on Aerospace and Electronic Systems.*, 2012, vol.48, no. 3, p. 2698 – 2710.
- [7] J. LI, X. WANG, L. QU, Calculation of Physical Optics Integrals Over NURBS Surface Using a Delaminating Quadrature Method, *IEEE Transactions on Antennas and Propagation*, 2012, vol. 60, no. 5, p. 2388 - 2397.